6th International Conference on Advances in Experimental Structural Engineering
11th International Workshop on Advanced Smart Materials and Smart Structures Technology
August 1-2, 2015, University of Illinois, Urbana-Champaign, United States

Condition assessment of long span cable-stayed bridges based on Structural Health Monitoring Techniques

Shunlong Li[1], Shaoyang He[2], Fujian Zhang[3], Hui Li[4]

1 *Associate Professor, School of Transportation Science and Engineering, Harbin Institute of Technology, Harbin, China.*
E-mail: lishunlong@hit.edu.cn
2 *Graduate Student, School of Transportation Science and Engineering, Harbin Institute of Technology, Harbin, China.*
E-mail: lishunlong@hit.edu.cn
3 *Senior Engineer, CCCC Highway Consultants CO., Ltd, Beijing, China.*
E-mail: sstl.illinois@gmail.com.
4 *Professor, School of Civil Engineering, Harbin Institute of Technology, Harbin, China.*
E-mail: lihui@hit.edu.cn

ABSTRACT
This paper presents long-term condition assessment approaches of cables and bridge decks under in-service loads based on Structural Health Monitoring (SHM) technique. Aiming to the critical structural components, three important issues related to the long term performance evaluation, including loads and responses modelling, resistance degradation and fatigue life assessment, were investigated in this study. For vehicle loads and responses modelling, the general homogeneous stochastic processwas employed to approximately simulate the monitored events. And a straightforward and general extreme value distribution model is derived by the Laplace transform. For the resistance degradation of cables, the deterioration process of steel wires considers simultaneously the uniform corrosion, pitting corrosion and the corrosion fatigue propagation, in which the cyclic stress was obtained through monitored cable forces. Based on the extension from steel wire deterioration to cable degradation, the cable reliability in terms of safety and serviceability incorporating the monitored responses and resistance degradation is further estimated. For fatigue life evaluation of the bridge decks, the accurate stress analysis of hot spot should be performed ahead taking advantage of multi-scale finite element model. The presented long term condition assessment of critical structural components would provide basis and guideline for the future maintenance and repair decision.

KEYWORDS: *Condition assessment; structural health monitoring; stochastic process; resistance degradation; fatigue evaluation*

1. GENERAL INSTRUCTIONS

Worldwide authorities on long-span bridges have recognized the importance of condition assessment in securing proper operation during the structure's lifetime. In the past decades, considerable efforts (Frangopol, 2011, Li, Bao, Li, Chen, Laima and Ou, 2013, Asadi, Da Silva, Antunes and Dias, 2012, Rainieri, Fabbrocino and Cosenza, 2011, Brownjohn, Xia, Hao and Xia, 2001) have been devoted to the condition assessment of long span bridges. For example, (Enright and Frangopol, 1999) presented the reliability-based condition assessment of deteriorating concrete bridges considering load redistribution. (Brownjohn, Xia, Hao and Xia, 2001) presented methodology for accurate and reliable condition assessment by finite element model updating. (Hua, 2006) studied the damage detection and model updating as well as damage alarming in his doctoral dissertation. (Asadi, Da Silva, Antunes and Dias, 2012) identified the most appropriate retrofitting options using the potential costs and impacts involved. (Rainieri, Fabbrocino and Cosenza, 2011) even incorporated seismic early warning and condition assessment together for critical civil infrastructures in seismically prone areas. However, at present the long-term conditions assessment of deteriorated long span bridges in operation is still limited and required for optimizing their inspection and replacement in real bridge maintenance practice.

This paper presents an investigation of the long-term condition assessment of two critical structural components (cables and the bridge decks) based on the installed SHM system. SHM systems collect massive amounts of in situ data enables the identification of traffic loads, cable forces and structural parameters (global and local), and the latter one could further be used in the updating of FEM. The directly measured traffic loads and cable forces acquired by SHM system are employed to estimate the extreme value distribution model of loads and responses. And then a coupled corrosion fatigue deterioration process of steel wires involving uniform corrosion, pitting corrosion and cyclic fatigue is taken into account using monitored cable forces. The reliability indices of the cable are evaluated in terms of the safety and serviceability criteria using the extreme value distribution model

of cable forces and probabilistic resistance degradation model. For the cumulative fatigue damage evaluation of bridge decks, it would be conducted by integrating the global and local finite element model together under the monitored traffic loading.

2. THE NANJING 3RD YANGTZE RIVER BRIDGE

The Nanjing 3rd Yangtze River Bridge, as shown in Figure 2.1, is one of the largest cable-stayed bridges constructed in the mainland of China. It comprises a main span of 648m and two side spans of 63+257 m each. The bridge tower is as high as 215m and consists 4 transverse beams. The tower below the bridge girder is made of pre-stressed concrete and the rest of the tower is made up of steel plates. There are totally 4×21 pairs of cables. Among the cables, the smallest number of 7mm steel wires consist in a cable is 109, while the largest of is 241.

Figure 2.1 Nanjing 3rd Yangtze River Bridge

During construction of the bridge, a sophisticated long-term structural health monitoring (SHM) system was designed and permanently implemented into the bridge in 2006. The SHM system incorporated a weigh-in-motion (WIM) system, accelerometers, temperature sensors, Inclinometer, pressure gauge and wind anemoscopes.

3. EXTREME VALUE DISTRIBUTION ESTIMATION OF LOADS AND RESPONSES

Maximum traffic activity, i.e., the extreme vehicle loads or loading response, is one of the most important aspects in the design and condition assessment of long-span bridges. To maintain the safety and serviceability of bridges, it is essential to investigate the extreme value distribution of the vehicle loads and loading responses of the bridges. Generally, the stochastic process of vehicle weights under normal operational conditions and peaks of loading responses could be simulated by homogeneous renewal processes.

3.1. Extreme value distribution for homogeneous renewal process

Given that the inter-arrival times T_n of a homogeneous renewal process are independent and identically distributed variables with the same probability density function $f_T(t)$, the pulse renewal process can be expressed as (Daley and Vere-Jones, 2007)

$$s(t)=\sum_{n=0}^{N(t)} x_n \cdot I(t,\tau_n),\ \ I(t,\tau_n)=\begin{cases}1, & t\in\tau_n\\ 0, & t\notin\tau_n\end{cases} \tag{3.1}$$

where x_n and τ_n denote the amplitude and duration time of the *n*th event, respectively, and $N(t)$ is the number of events in the interval [0, *t*].

Considering that the inter-arrival times might not follow a well-known distribution, the extreme value distribution estimation methodology for general homogeneous renewal processes is proposed in this study. The cumulative distribution function of the extreme value, i.e., $\max\{s(t),t\in[0,T]\}$ can be determined by

$$F_{\mathrm{MN}}(x;T)=P(\max\{s(t),t\in[0,T]\}\le x) \tag{3.2}$$

$$= \sum_{n=0}^{\infty} P\left(\max\left\{s(t), t \in [0,T]\right\} \le x \mid N(t) = n\right) P\left(N(t) = n\right)$$
$$= \sum_{n=0}^{\infty} P(x_1 \le x, x_2 \le x, \cdots, x_n \le x) P\left(N(t) = n\right)$$

The probability $P\left(N(t) = n\right)$ can be calculated using

$$\begin{aligned} & P\left(N(t) = n\right) = P\left(N(t) \ge n\right) - P\left(N(t) \ge n+1\right) \\ & = \underbrace{F_T(t) * \cdots F_T(t)}_{n} - \underbrace{F_T(t) * \cdots F_T(t)}_{n+1} \\ & = \mathrm{C}\left[F_T(t), n\right] - \mathrm{C}\left[F_T(t), n+1\right] \end{aligned} \tag{3.3}$$

where $F_T(t)$ is the cumulative distribution function (CDF) of the inter-arrival times, the symbol $*$ denotes convolution, and $\mathrm{C}\left[F_T(t), n\right]$ is the convolution of $F_T(t)$ for *n* times. Considering that the event amplitude x_n are independent and identically distributed with $F_{\mathrm{N}}(x)$, Eq. (3.3) can be transformed into

$$\begin{aligned} & F_{\mathrm{MN}}(x;T) = \sum_{n=0}^{\infty} \left[F_{\mathrm{N}}(x)\right]^n \left\{\mathrm{C}\left[F_T(t), n\right] - \mathrm{C}\left[F_T(t), n+1\right]\right\} \\ & = \mathrm{C}\left[F_T(t), 0\right] - \mathrm{C}\left[F_T(t), 1\right] + F_{\mathrm{N}}(x)\mathrm{C}\left[F_T(t), 1\right] - F_{\mathrm{N}}(x)\mathrm{C}\left[F_T(t), 2\right] \cdots \\ & = \mathrm{C}\left[F_T(t), 0\right] - \sum_{n=1}^{\infty} \left[1 - F_{\mathrm{N}}(x)\right] \left[F_{\mathrm{N}}(x)\right]^{n-1} \mathrm{C}\left[F_T(t), n\right] \end{aligned} \tag{3.4}$$

Performing the Laplace transform on both sides of Eq. (3.4) results in

$$\begin{aligned} & \mathcal{L}\left(\mathrm{C}\left[F_T(t), n\right]\right) = \frac{1}{\ell} \mathcal{L}\left\{\mathrm{C}\left[f_T(t), n\right]\right\} = \frac{1}{\ell}\left[\mathcal{L}\left\{f_T(t)\right\}\right]^n \\ & \mathcal{L}\left(F_{\mathrm{MN}}(x;T)\right) = \mathcal{L}\left(\mathrm{C}\left[F_T(t), 0\right]\right) - \sum_{n=1}^{\infty} \left[1 - F_{\mathrm{N}}(x)\right] \left[F_{\mathrm{N}}(x)\right]^{n-1} \mathcal{L}\left(\mathrm{C}\left[F_T(t), n\right]\right) \\ & = \frac{1}{\ell} \mathcal{L}\left(f_T(t)\right)^0 - \frac{1}{\ell} \cdot \frac{1 - F_{\mathrm{N}}(x)}{F_{\mathrm{N}}(x)} \cdot \sum_{n=1}^{\infty} \left[F_{\mathrm{N}}(x)\right]^n \mathcal{L}\left(f_T(t)\right)^n \\ & = \frac{1}{\ell} - \frac{1}{\ell} \cdot \frac{1 - F_{\mathrm{N}}(x)}{F_{\mathrm{N}}(x)} \cdot \frac{F_{\mathrm{N}}(x)\mathcal{L}\left(f_T(t)\right)}{1 - F_{\mathrm{N}}(x)\mathcal{L}\left(f_T(t)\right)} \\ & = \frac{1 - \mathcal{L}\left(f_T(t)\right)}{\ell\left\{1 - F_{\mathrm{N}}(x)\mathcal{L}\left(f_T(t)\right)\right\}} \end{aligned} \tag{3.5}$$

where the symbol $\mathcal{L}(\cdot)$ denotes the Laplace transform, and $f_T(t)$ represents the probability density function (PDF) of the inter-arrival times. The extreme value distribution function for homogeneous renewal process can then be expressed by

$$F_{\mathrm{MN}}(x;T) = \mathcal{L}^{-1}\left(\frac{1 - \mathcal{L}\left(f_T(t)\right)}{\ell\left\{1 - F_{\mathrm{N}}(x;T)\mathcal{L}\left(f_T(t)\right)\right\}}\right) \tag{3.6}$$

Eq. (3.6) indicates that the expression of the extreme value distribution can be uniquely determined by the PDF of the inter-arrival times $f_T(t)$ and the CDF of the event amplitudes $F_{\mathrm{N}}(x)$.

For the investigated bridge, the predicted weekly extreme value distributions, calculated from Eq. (3.6), followed the Gumbel distribution and are shown in Figure 3.1(a). It can be seen from Figure 3.1(a) that the predicted extreme value distribution by the proposed method is consistent with the observed distribution, which validates the proposed method. However the predicted extreme value distribution by the Code recommended method deviated far away from the observed distribution. Figure 3.1(b) shows the extreme value distributions of

the vehicle weights at different operational periods. Both the mean value and the standard deviation of the extreme vehicle weights increased with the increase in the operational period.

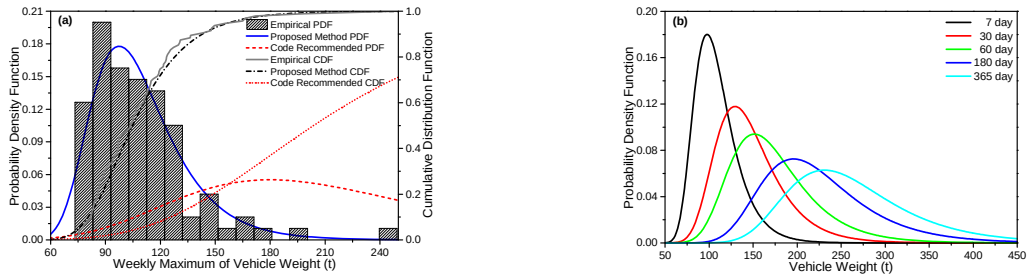

Figure 3.1 Vehicle weights in the normal state: (a) Comparison of observed and predicted weekly extreme value distributions; (b) Extreme value distribution prediction at different operational periods.

3.2. Cable force modelling

Figure 3.2 Illustrates the typical cable force time history during March 1 0:00-March 7 0:00, 2012. The selected stay cable consists of 151 steel wires that have a diameter of 7 mm and a length of LC = 150.24 m. The total cross sectional area of the stay cable is 58.112 cm2. It could be seen from the figure that the cable force fluctuation mainly consists of dead load effects and vehicle load effects and the temperature has limit influence on the cable force variation compared to the vehicle load effects.

Similar to the vehicle load modeling, the inter-arrival times could be fitted by gamma distribution, $\Gamma(k,\theta)$, where the scale parameter, θ=10.21, and the shape parameter, $k=2.68$, are obtained from the monitored cable force. The the scale parameter θ and the shape parameter k do not necessarily consistent with the vehicle modelling, for the there were certain distances between vehicle load and cable force monitoring location.

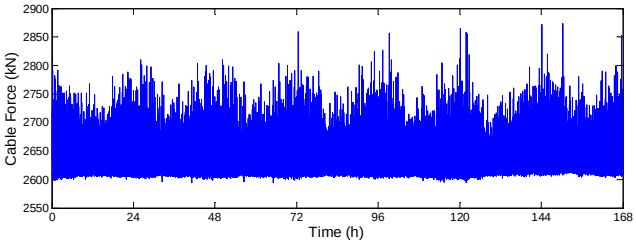

Figure 3.2 Monitored Cable Force (March 1 0:00-March 7 0:00, 2012)

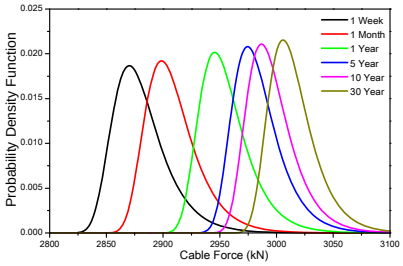

Figure 3.3 Extreme value distribution prediction at different operational periods

The exceedance in cable force above the threshold U_N can also be fitted by the generalised Pareto distribution and the extreme value distribution under different calculation period would be generated by the Eq. 3.6, using the same computing process as the vehicle load modelling, shown in Figure 3.3

4. SERVICEABILITY AND SAFETY ASSESSMENT OF DETERIORATED CABLES

Bridge inspections reveal that severe corrosion and fatigue are the main failure mechanisms of bridge stay cables. Through accelerated corrosion tests, (Li, Xu, Li and Guan, 2014) illustrated the uniform and pitting corrosion characteristics of high-strength steel wires. The time-dependent statistical model of uniform corrosion depth can be expressed as

$$\begin{aligned} a_u(t) &= a_{u,\mathrm{Zn}}(t) = \psi_1 t^{\gamma_1} && t \le t_c \\ a_u(t) &= a_{u,\mathrm{Zn}}(t_c) + a_{u,\mathrm{Fe}}(t) = a_{u,\mathrm{Zn}}(t_c) + \psi_2 (t - t_c)^{\gamma_2} && t > t_c \end{aligned} \tag{4.1}$$

where $a_u(t)$, $a_{u,\mathrm{Zn}}(t)$ and $a_{u,\mathrm{Fe}}(t)$ denote the total uniform corrosion depth, the uniform corrosion depth of the zinc coating, and the uniform corrosion depth of steel, respectively (unit: μm); t_c represents the critical

time at which the zinc coating is completely consumed and the steel starts to corrode; $a_{u,\mathrm{Zn}}(t_c)$ denotes the zinc coating thickness; ψ_1 and γ_1, ψ_2 and γ_2 are four parameters determining the uniform corrosion depth. And the maximum pitting corrosion depth $a_p(t)$ can be approximately estimated by

$$a_{\mathrm{p}}(t) = \Lambda_m a_{u,\mathrm{Fe}}(t), \quad t > t_c \tag{4.2}$$

where the Λ_m indicates the pitting factor that can be described by a Gumbel extreme value distribution (Stewart, 2009). The corresponding cumulative distribution function and the parameters are obtained by (Li, Xu, Li and Guan, 2014)

$$F_{\Lambda_m}(x) = \exp\left[-\exp\left(-\frac{x-\beta_\kappa}{\alpha_\kappa}\right)\right] \tag{4.3a}$$

$$\hat{\alpha}_\kappa = 0.954, \hat{\beta}_\kappa = 0.905\ln\left(\frac{A_\kappa}{A_0}\right) + 4.078 \tag{4.3b}$$

where A_0 is the surface area of a steel wire with a diameter of 7mm and a length of 21mm; α_κ and β_κ denote the scale and location parameter with surface area A_κ. Then the time-dependent uniform and pitting corrosion models are further extended to estimate the crack growth induced by corrosion fatigue, an environmentally assisted fatigue situation. Based on the test results of high-strength steel wires, (Huneau and Mendez, 2006) suggested to evaluate corrosion fatigue crack growth using Paris-Erdogan law (Paris and Erdogan, 1963)

$$\frac{da_{\mathrm{f}}}{dN} = C\Delta K^m \tag{4.5}$$

where da_{f}/dN indicates the crack growth rate; m represents the Paris Exponent; $\Delta K = K_{\max} - K_{\min}$ demonstrates the stress intensity factor range, C is crack growth rate. In this study, the stress range in the steel wires can be estimated based on the real-time monitoring of cable forces, shown in Figure 3.2.

Figure 4.1 illustrates the crack evolution of the steel wires over time, including the mean value and standard deviation of the crack depth, and the mean value of the ratio (or percentage) of broken wires. It can be seen that all three variables increase nonlinearly over time. Kolmogorov Smirnov (K-S) Hypothesis Testing at significance level of 5% indicates that the distribution of crack depth shown in Figure 4.1 does not reject the lognormal distribution. The statistical models of mechanical properties for corroded wires could be established based on tensile experiment and the relationship between the corrosion fatigue crack depth and the mechanical properties were obtained. The time-variant conditions of bridge cables (sectional area loss and remaining capacity) would be probabilistically assessed, as shown in Figure 4.2.

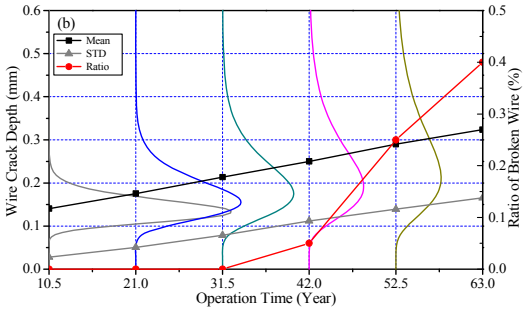

Figure 4.1 Evolution of wire crack depth and broken wire ratio

According to China's Technical Code of Maintenance for City Bridge (J281-2003), the cable should be replaced when the loss of cable's cross sectional area caused by corrosion exceeds 10%. Considering the time-variant

distributions of cross sectional area loss, as shown in Figure 4.2(a), the long-term serviceability reliability is assessed in Figure 4.3(a). The reliability index β drops considerably in the early service period, while the deterioration speed would become slow in the subsequent service period. The reliability index of the serviceability of the cable is less than 2 after 30-year service.

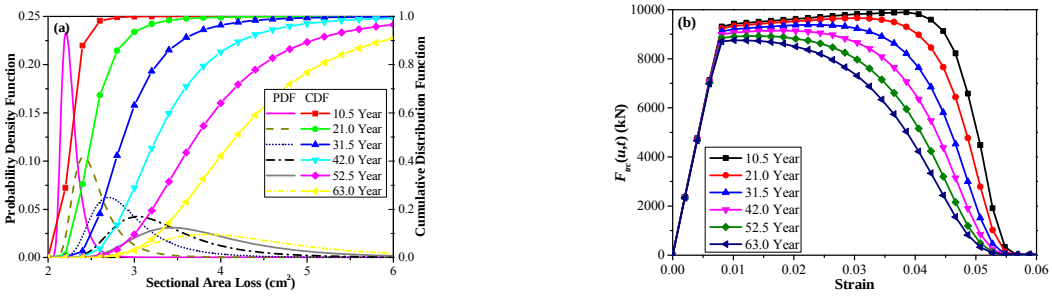

Figure 4.2 Evolution of properties of corroded stay cable: (a) sectional area loss; and (b) average relationship between cable force and cable strain

For the safety assessment, the extreme value distribution of cable forces shown in Figure 3.3 and the resistance degradation shown in Figure 4.2(b) were taken into account. The reliability index β of cable safety can be determined as a function of operation time, shown in Figure 4.3(b). For the investigated cable, at the end of the service period, the smallest reliability index is estimated to be higher than 41, implying an excellent safety margin under the extreme traffic loads during the entire design life. However, the reliability in terms of the serviceability limit state is much lower than that of the safety limit state. Thus the maintenance and replacement of the cables will be likely governed by the serviceability criterion if applied.

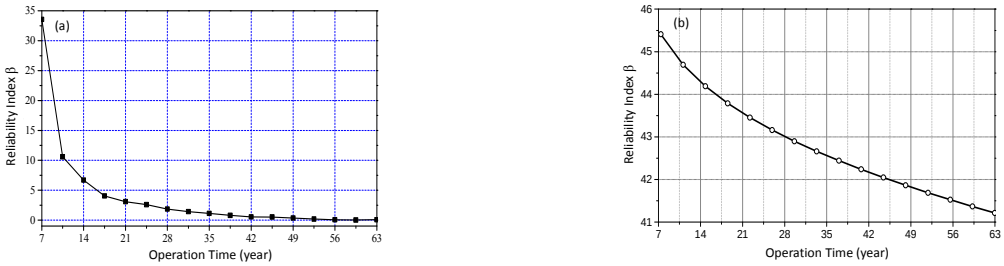

Figure 4.3 Long-term (a) serviceability and (b) safety reliability analysis.

5. FATIGUE DAMAGE EVOLUTION OF STEEL BRIDGE DECKS BASED ON MULTI-SCALE FINITE ELEMENT MODELING

In this study, a three-dimensional finite element model (shown in Figure 5.1) was constructed according to the engineering drawings with ANSYS program in order to estimate the global dynamic and static characteristics. The finite element model of Nanjing 3rd Yangtze River Bridge consists of 1172 BEAM188 elements, 873 MASS21 elements, 168 LINK10 elements, 12 COMBIN14 elements.

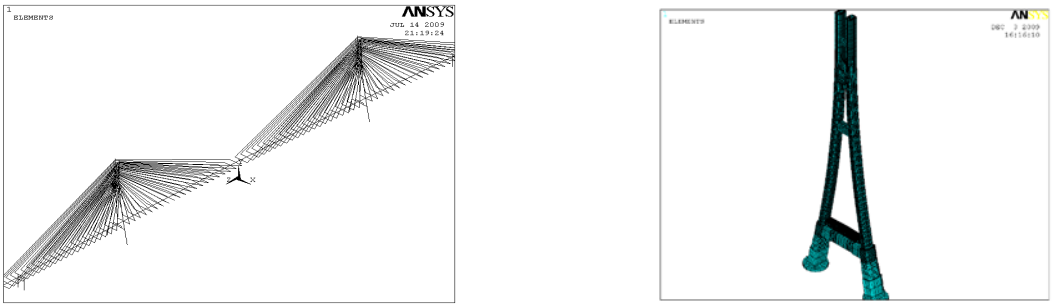

Figure 5.1 Three dimension FEM of the cable-stayed bridge

The welded regions or notches at the upper flange of bridge decks, where the local stress is concentrated due to the wheel partial pressure, are vulnerable to fatigue damage. To conduct the fatigue evaluation, the stress of

these local areas would be required and obtained by structural health monitoring technique or finite element analysis. However, there is no effective instrument for welded regions or notches stress testing at present; Also the above global finite element model can not obtain the stress time history in the local area. In this paper, the local finite element model of bridge deck is incorporated into the aforementioned global finite element model to calculate the hot spot stress for fatigue damage and the remaining life prediction. The tires pressure surface would be also considered in the local finite element model.

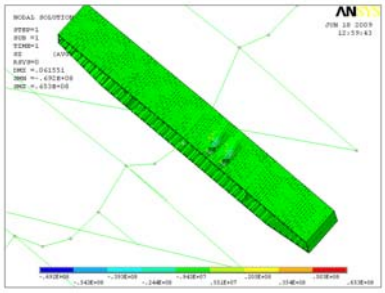

Figure 5.2 Stress analysis results of multi-scale finite element model

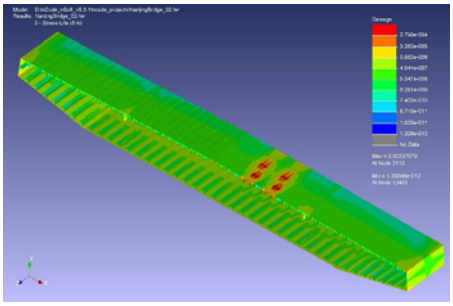

Figure 5.3 Evolution of fatigue accumulative damage of bridge deck

The monitored 4 year vehicle loads were selected as loading cycle block and supposed to repeat in the subsequent service period. The stress range at the local areas can be obtained by integrating the stress analysis of multi-scale finite element model and monitored fatigue vehicle load cycle together. The stress range ΔS and number of cycles to failure N satisfies the following empirical relationship

$$\Delta S^m N = C \tag{5.1}$$

where C and m are constants related to the material. Based on the BS5400 fatigue strength grade D' for the steel plates, C is equal to 1.52×10^{12} and m is equal to 3.0. Considering the monitored traffic volume, the damage index based on Palmgren-Miner rule (Hashin, 1980) can be calculated and the fatigue accumulative damage evolution of bridge deck is shown in Figure 5.3. It can be seen from Figure 5.3 that the damage index of bridge deck under local tire pressure was much larger than that of other areas, thus the fatigue accumulative damage of the upper flange of the bridge deck was much more severe than that of lower flange. Furthermore, the accumulative damage index would not be higher than the 1 even for vulnerable areas if suffered from monitored traffic loading during the service life.

6. CONCLUSION

In this study, the long-term condition assessment for the two critical structural components: cables and bridge decks, were performed based on structural health monitoring techniques. The following conclusions were drawn from the results of the study.

(1) A general extreme value distribution model for gamma process with non-integer shape parameter is derived by the Laplace transform. The extreme value distribution of SHM-monitored traffic loads and cable forces would be evaluated in different operation periods by modelling monitored events with gamma processes. The comparison between the predicted extreme value distribution and the observed distribution shows the effectiveness of the proposed general extreme value distribution model.

(2) The life-cycle reliability of the cable in terms of the serviceability and safety is computed and discussed based on the time-variant conditions of the cables (the loss of cross sectional area and the remaining resistance), where the time-dependent probabilistic models of investigated cables are established by incorporating the experimental results, tensile test results of the corroded wires, and real-time monitoring data of cable stress. The safety reliability index shows a good safety margin in comparison with the monitored cable forces under traffic loads, while the serviceability index implies the necessary periodic maintenance and replacement in the service life.

(3) The multi-scale finite element model of bridge decks suffered from complicated stress concentration were established, in which the global finite element model was first updated according to the identified modal parameters and cable forces. The 4 year monitored traffic loads were selected as the loading cycle block and the fatigue accumulative damage proved fatigue safety of bridge decks in the service life.

The long-term condition assessment of cables and bridge decks based on the structural health monitoring techniques can improve predictions of deterioration over the service life and guide future decision-making on bridge maintenance and repair.

ACKNOWLEDGEMENTS
Financial support for this study was provided by Ministry of Science and Technology of the People's Republic of China (MOST, Grant No. 2014AA110401, 2013CB036305 and 2011CB013604), National Natural Science Foundation of China (NSFC, Grant No. 51478149) and Postdoctoral Scientific Research Development fund of Heilongjiang Province (Grant No. LBH-Q14081).

REFERENCES

[1] Frangopol, D. M. (2011). Life-cycle performance, management, and optimisation of structural systems under uncertainty: accomplishments and challenges. *Structure and Infrastructure Engineering*, **7(6)**, 389-413.
[2] Li, H., Bao, Y. Q., Li, S. L., Chen, W. L., Laima, S. J., and Ou, J. P. (2013). Monitoring, Evaluation and Control for Life-Cycle Performance of Intelligent Civil Structures. *Advances in Science and Technology*, **83**, 105-114.
[3] Asadi, E., Da Silva, M. G., Antunes, C. H., and Dias, L. (2012). Multi-objective optimization for building retrofit strategies: a model and an application. *Energy and Buildings*, **44**, 81-87.
[4] Rainieri, C., Fabbrocino, G., and Cosenza, E. (2011). Integrated seismic early warning and structural health monitoring of critical civil infrastructures in seismically prone areas. *Structural Health Monitoring*, **10(3)**, 291-308.
[5] Brownjohn, J. M., Xia, P.-Q., Hao, H., and Xia, Y. (2001). Civil structure condition assessment by FE model updating: methodology and case studies. *Finite Elements in Analysis and Design*, **37(10)**, 761-775.
[6] Enright, M. P., and Frangopol, D. M. (1999). Reliability-based condition assessment of deteriorating concrete bridges considering load redistribution. *Structural Safety*, **21(2)**, 159-195.
[7] Hua, X. (2006). Structural health monitoring and condition assessment of bridge structures. Doctoral Dissertation, The Hong Kong Polytechnic University.
[8] Daley, D. J., and Vere-Jones, D. (2007). *An introduction to the theory of point processes: volume II: general theory and structure*, Springer Science & Business Media.
[9] Snyder, D. L. (1975). *Random point processes*, Wiley.
[10] Li, S., Xu, Y., Li, H., and Guan, X. (2014). Uniform and Pitting Corrosion Modeling for High-Strength Bridge Wires. *Journal of Bridge Engineering*, **19(7)**, 04014025.
[11] Stewart, M. G. (2009). Mechanical behaviour of pitting corrosion of flexural and shear reinforcement and its effect on structural reliability of corroding RC beams. *Structural safety*, **31(1)**, 19-30.
[12] Huneau, B., and Mendez, J. (2006). Evaluation of environmental effects on fatigue crack growth behaviour of a high strength steel in a saline solution with cathodic protection. *International journal of fatigue*, **28(2)**, 124-131.
[13] Paris, P., and Erdogan, F. (1963). A critical analysis of crack propagation laws. *Journal of Fluids Engineering*, **85(4)**, 528-533.
[14] Hashin, Z. (1980). A reinterpretation of the Palmgren-Miner rule for fatigue life prediction. *Journal of Applied Mechanics*, **47(2)**, 324-328.